Desalination and Water Treatment
www.deswater.com

doi: 10.1080/19443994.2015.1033473

57 (2016) 2489–2502
February

Taylor & Francis
Taylor & Francis Group

Photodegradation of olive mill effluent with hydrogel-coated Fe_3O_4 magnetite composite

Delia Teresa Sponza*, Rukiye Oztekin

Engineering Faculty, Department of Environmental Engineering, Dokuz Eylül University, Tınaztepe Campus, Buca, 35160 İzmir, Turkey, Tel. +90 232 412 71 19; Fax: +90 232 453 11 43; emails: delya.sponza@deu.edu.tr (D. Teresa Sponza), rukiyeoztekin@gmail.com (R. Oztekin)

Received 14 September 2014; Accepted 17 March 2015

ABSTRACT

In this study, hydrogel-coated Fe_3O_4 magnetite composite was used for the photocatalytic degradation of pollutant parameters [polyphenols, chemical oxygen demand (COD) components, total aromatic amines (TAAs)] from the olive mill effluent wastewater at different pH (4.0–7.0–9.0) conditions, at temperatures (21, 30, and 40˚C), at different H_2O_2 concentrations (50, 100, 200, and 1,000 mg/l), at different retention times (15, 30, 45, and 60 min), and increasing hydrogel-coated Fe_3O_4 magnetite composite concentrations under 100 W ultraviolet (UV) and 29 W sunlights. The maximum COD_{total}, polyphenols, and TAAs yields were 96%, at between 88 and 94%, and at between 83 and 94%, respectively, at 3 g/l of hydrogel-coated Fe_3O_4 magnetite nano composite concentration, at 100 W UV light irradiation, at pH 4.0, after 60 min retention time, respectively. At the lowest molar ratio of 1/5 in the iron(II) chloride tetrahydrate and iron(III) chloride hexahydrate to hydrogel the highest photodegradation obtained at 30˚C. When the molar ratio of the iron(II) chloride tetrahydrate and iron(III) chloride hexahydrate to hydrogel was 1/3 to the maximum photodegradation reached at 40˚C. At the higher molar ratio of 1/2, the best photodegradation yields were obtained at 40˚C. The maximum COD_{total}, polyphenols, and TAAs yields were obtained at acidic pH, and at 50 mg/l H_2O_2 concentration. The Fe_3O_4 nanoparticles exhibited high catalytic recyclability under magnetic conditions resulting in significant decrease in treatment costs.

Keywords: Total aromatic amines; Hydrogel-coated Fe_3O_4 magnetite composite; H_2O_2; Magnetic separation process; Olive mill effluent wastewater; Photocatalytic degradation; Polyphenols; Sunlight; Ultraviolet

1. Introduction

Hydrogels are three-dimensional hydrophilic polymers capable of absorbing and retaining water (H_2O) without disintegrating [1,2]. In recent years, polymer hydrogels have also generated great interests in the application of different areas such as pollutant removal, biosensors, artificial muscles, and drug delivery devices, due to their versatility and stimulus-responsive properties [3–5]. Hydrogel are widely used

*Corresponding author.

Presented at the 2nd International Conference on Recycling and Reuse (R&R2014), 4–6 June 2014, Istanbul, Turkey

in the purification of wastewater: Various hydrogels were synthesized and their adsorption behavior for heavy metals was investigated. Kesenci et al. was prepared poly(ethyleneglycol dimethacrylate-coacrylamide) hydrogel beads for the adsorptions of Pb(III), Cd(II), and Hg(II) [6]; Essawy and Ibrahim prepared poly(vinylpyrrolidone-co-methylacrylate) hydrogel for removals of Cu(II), Ni(II), and Cd(II) via adsorption [7]; while Barakat and Sahiner, prepared poly(3-acrylamidopropyl)trimethyl ammonium chloride hydrogels for As(V) removal [8]. The removal is basically governed by the H_2O diffusion into the hydrogel, carrying the heavy metals inside, especially in the absence of strongly binding sites [8,9]. However, the use of hydrogels in several applications is limited since most of them are brittle, soft, and typically exhibit low mechanical strength and poor stability [10]. To solve this problem, intense efforts are devoted to synthesizing hydrogels with improved mechanical properties. As a pioneering example, clay nanocomposite hydrogel shows ultrahigh tensile strength and elongation due to the multiple non-covalent effects between mono-dispersed clay nanosheets and polyacrylamide chains [11–14]. Wang et al. has developed the supramolecular hydrogel by mixing sodium polyacrylate dispersed clay nanosheets with dendritic polymers via multiple salt bridges [15]. Nevertheless, no much information is available on the functionalization of high strength hydrogel for practical applications. Recently, the fabrication and magnetic characterization of iron-oxide (γ-Fe_3O_4) nanoparticles precipitated inside the hydrogel beads have been reported. Hydrogels are promising materials used for biomedical applications due to their bio-similarity, aqueous environment, porous structure, and facility of conjugation with various biological macromolecules [16]. The alginate hydrogel beads could protect the basic-sensitive pollutants from the wastewaters [16]. The alginate-hydrogel composite containing γ-Fe_3O_4 was prepared as a pH depending treatment process to protect environment from the pollutants. Hydrogel-metal nanocomposites offer an interesting environment for many applications including catalysis for the treatment of refractory wastewaters [16]. This attention is warranted because these hydrogels are stable at different wide pH intervals (pH 3.0–11.0) [17,18]. The high surface to volume ratio of magnetite (Fe_3O_4) nanoparticles, however, results with aggregation of them. For exploitation of their intrinsic magnetic properties, the surface of these nanoparticles is usually modified using polymers co-polymers and hydrogel to improve their stability and dispersibility as catalyst. The photocatalytic performance of Fe_3O_4 nanoparticles was related to the pH-responsive swelling of polymer hydrogel [16]. The polymeric structure prevented the aggregation of Fe_3O_4, thus providing larger surface area of the hydrogel-coated Fe_3O_4 magnetite composites. The hydrophilic structure of hydrogel facilitated contact between the pollutants and the catalyst which could improve the diffusion of reactants [16]. In addition to the hydrogel polymer, it can effectively reduce the overall cost of adsorbent because of its high adsorption capacity, good separation selectivity and excellent reusing ability [16].

Olive mill effluent wastewater (OMW) arising from olive processing is one of the strongest industrial effluents, with chemical oxygen demand (COD) values of up to 220 g/l and corresponding biochemical oxygen demand 5 d (BOD_5) values of up to 100 g/l [19–21]. The wastewater arising from the milling process amounts to 0.5–1.5 m^3 per 1,000 kg of olives depending on the process. The characteristics of OMW are variable, depending on many factors such as method of extraction, type, and maturity of olives, region of origin, climatic conditions, and associated cultivation/processing methods. Besides its strong organic content [BOD_5 = 35–110 g/l, COD = 45–170 g/l, total suspended solids (TSS) = 1–9 g/l, respectively]. OMW contains high concentrations of recalcitrant compounds such as lignins and tannins which give it a characteristic dark color (52,270–180,000 mg/l Pt-Co units), but, most importantly, it contains phenolic compounds and long-chain fatty acids which are toxic to micro-organisms and plants [21]. The phenolic compounds can be either simple phenols and flavonoids, or polyphenols which result from polymerization of the simple phenols. The concentration of phenolic compounds in OMW varies greatly from 0.5 to 24 g/l [20,22]. The high recalcitrant organic load and the associated toxicity make the treatment of OMW imperative.

In this study, the effects of increasing concentrations of hydrogel-coated Fe_3O_4 magnetite composites (1, 3, 5 and 7 g/l) on the pollutant parameters of OMW [polyphenols (2-phenyl-phenol, 3-phenyl-phenol, catechol, 4-methyl catechol), COD components (COD_{total}, $COD_{dissolved}$, COD_{inert}), total aromatic amines (TAAs) metabolites (2,4,6 trimetylaniline, aniline, o-toluidine, o-anisidine, dimethylaniline, ethylbenzene)] were studied at the different pH levels (4.0–7.0–9.0), at different H_2O_2 concentrations (50, 100, 200, and 1,000 mg/l), at different retention times (15, 30, 45, and 60 min), at different temperatures (21, 30, and 40°C) under ultraviolet (UV) (100 W) and sun (29 W) light irradiations. Furthermore, the effects of decreasing molar ratio of the iron(II) chloride tetrahydrate and iron(III) chloride hexahydrate to hydrogel in the hydrogel-coated Fe_3O_4 magnetite composites to

the photodegradation of pollutants in the OMW at increasing temperatures.

2. Materials and methods

2.1. Used chemicals

Hydrogel, iron(II) chloride tetrahydrate (cas no: 13478-10-9), iron(III) chloride hexahydrate (cas no: 10025-77-1) and ammonium persulfate (cas no: 7727-54-0), sodium hydroxide (≥98%) (cas no: 1310-73-2), sulfuric acid (H_2SO_4) (95–98%) (cas no: 7664-93-9), ethanol (cas no: 64-17-5), and butanol (cas no: 71-36-3) were purchased from Merck, (Germany) while reagent grade N,N_1-methylenebisacrylamide (≥99%) (cas no: 110-26-9) was obtained from Fluka, (Germany). N_2 (99.98%) was purchased from Linde, (Germany). Catechol (99%) (cas no: 120-80-9), tyrosol (99%) (cas no: 501-94-0), quercetin (99%) (cas no: 6151-25-3), caffeic acid (99%) (cas no: 331-39-5), 4-methyl catechol (99%) (cas no: 62-32-8), 2-phenyl-phenol (2-PHE) (99%) (cas no: 287389-48-4), 3-phenyl-phenol (3-PHE) (99%) (cas no: 768-25-1), 2,4,6 trimetylaniline (99%) (cas no: 88-05-1), aniline (99%) (cas no: 62-53-3), o-toluidine (99%) (cas no: 95-53-4), o-anisidine (99%) (cas no: 90-04-0), dimethylaniline (99%) (cas no: 87-62-7), and ethylbenzene (99%) (cas no: 100-41-4) were purchased from Aldrich, (Germany).

2.2. Configuration of kuvars glass reactors used in the photocatalytic studies

A 3-l kuvars glass reactor was used for the experimentation. An UV lump with a power of 100 W was placed inside reactor with a separated volume of in the center of the reactor. In the studies with sun light the kuvars glass reactors containing 2-l OMW was under sunlight; at the maximum sunlight obtained between 11.00 and 15.00 h during a day. The temperature increase from 21˚C up to 30 and 40˚C with a peristaltic pump pumping the hot water around the glass reactor with an automatic heat exchanger.

2.3. Preparation of hydrogel-coated Fe_3O_4 magnetite composite in laboratory conditions

Hydrogel was synthesized from acrylamide. Fig. 1 shows three-dimensional network formation of cationic hydrogel [8]. Ammonium persulfate, N,N_1-methylenebisacrylamide and N_2(g) were used to prepare the hydrogel. The hydrogel was reacted with iron (II) chloride tetrahydrate, iron(III) chloride hexahydrate in the presence of ammonium hydroxide to prepare hydrogel-coated Fe_3O_4 magnetite composites. Different iron(II) chloride tetrahydrate and iron(III) chloride hexahydrate (molar ratio of 1/2, 1/3, 1/4, 1/5) with respect to the hydrogel were prepared.

2.4. Operational conditions

The COD components, polyphenols and TAAs metabolites yields in the OMW were determined at increasing hydrogel-coated Fe_3O_4 magnetite composite concentrations (1, 3, 5, and 7 g/l), at increasing pH levels (4.0–7.0–9.0) and increasing H_2O_2 concentrations (50, 100, 200, and 1,000 mg/l) at different retention times (15, 30, 45, and 60 min) under photocatalytic conditions (100 W UV and 29 W sunlights). The pH of the OMW was adjusted using 0.2 N NaOH and 0.2 N H_2SO_4.

2.5. Analytical methods

pH, T(˚C), ORP, DO, BOD_5, COD_{total}, $COD_{dissolved}$, TSS, Total-N, NH_3-N, NO_3-N, NO_2-N, Total-P, and PO_4-P measurements were monitored following the Standard Methods 2,310, 2,320, 2,550, 2,580, 4,500-O, 5,210 B, 5,220 D, 2,540 D, 4,500-N, 4,500-NH_3, 4,500-NO_3, 4,500-NO_2, and 4,500-P [23]. Inert COD was measured according to glucose comparison method [24]. Trimethlyaniline, aniline, o-toluidine, o-anisidine, dimethylaniline, and ethylbenzene were identified as TAAs were identified with a high-pressure liquid chromatography (HPLC) (Agilent-1,100) with a C-18 reverse phase HPLC column, (25 cm × 4.6 mm × 5 μm, (Ace5C-18). o-anisidine was measured in a HPLC (Agilent-1100) with a UV detector at a mobile phase of 35% acetonitrile/65% H_2O at a flow rate of 1.2 ml/min. Total phenol, 2-PHE, 3-PHE, catechol, and 4-methyl catechol (HPLC, Agilent-1100) with a Spectra system model SN4000 pump and Asahipak ODP-506D column (150 cm × 6 mm × 5 μm). A scanning electron microscopy (SEM) (Hitachi S-4800 N), a Fourier transform infrared spectroscopy (FTIR) (Nicolet 5700, America) and an X-ray diffraction (XRD) diffractometer (Bruker AXS, Germany) is were used to detect the structural changes of hydrogel-coated Fe_3O_4 magnetite composites after photocatalytic degradation with UV and sun light irradiations.

All experiments were carried out three times and the results given as the means of triplicate samplings.

3. Results and discussion

3.1. Characterization of raw OMW

The characterization of raw OMW taken from the influent of an olive mill effluent in İzmir, Turkey is

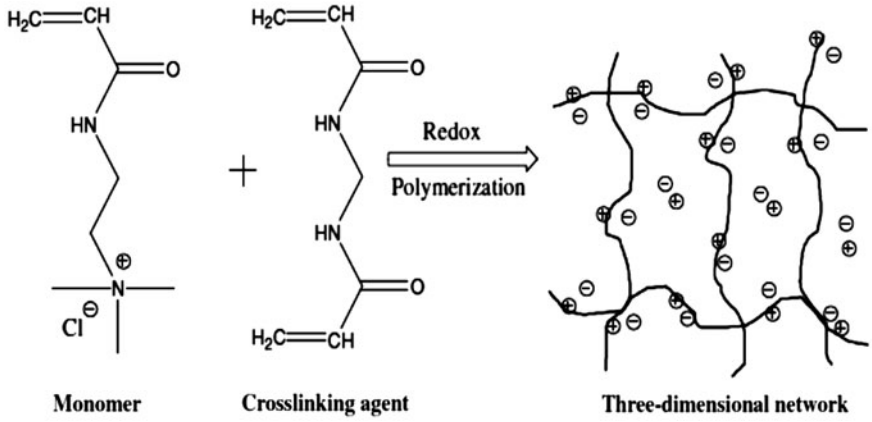

Fig. 1. Three-dimensional network formation of cationic hydrogel [8].

given in Table 1. This plant is operated with a three-phase olive oil extraction process.

3.2. SEM, FTIR, and XRD analysis results of the hydrogel and hydrogel-coated Fe_3O_4 magnetite composite produced in laboratory conditions

3.2.1. FTIR analysis results

The FTIR analysis results for hydrogel, Fe_3O_4 nanoparticles and hydrogel-coated Fe_3O_4 magnetite composites were shown in Fig. 2(a), (b), and (c), respectively. Common peaks were observed at 2,500, 2090, and 1,060 1/cm due to the presence of amide and carbonyl groups in the gel structure. An addition peak at 610 1/cm was observed in the case of Fe_3O_4 nanoparticles (Fig. 2(b)). This is a common stretching peak observed for Fe–O vibrations of Fe_3O_4 nanoparticles.

3.2.2. XRD analysis results

Fig. 3 showed the XRD analysis results for hydrogel (a), Fe_3O_4 nanoparticles (b) and hydrogel-coated Fe_3O_4 magnetite composites (c), respectively. To study the crystallographic nature of Fe_3O_4 nanoparticles and the hydrogel-coated Fe_3O_4 magnetite composites XRD analysis was performed. Hydrogel (Fig. 3(a)) and Fe_3O_4 nanoparticles (Fig. 3(b)) have not exhibited any sharp peak in XRD. The hydrogels shows a broad peak at 2θ (Fig. 3(a)) due to the polymer network. In the case of hydrogel-coated Fe_3O_4 magnetite composites (Fig. 3(c)), sharp peaks are observed at $2\theta = 29.9^\circ$, 35.03°, 42.6°, 51.2°, 56.8°, and 65.3°. The XRD patterns indicate that the formation of highly crystalline Fe_3O_4 nanoparticles and the prepared nanoparticles are pure Fe_3O_4 with an inverse cubic spinel structure, which is identical to the standard XRD patterns of Fe_3O_4 nanoparticles.

3.2.3. SEM analysis results

Fig. 4(a) shows the SEM analysis results for hydrogel-coated Fe_3O_4 magnetite composites in OMW without photocatalytic treatment and after photocatalytic treatment (Fig. 4(a) and (b), respectively). The hydrogel-coated Fe_3O_4 magnetite composite covered with COD, TAAs, and plyphenol pollutants in the OMW during photocatalytic treatment (Fig. 4(b)).

3.3. Effects of molar ratios of iron(II) chloride tetrahydrate and iron(III) chloride hexahydrate (1/2, 1/3, 1/4, and 1/5) to hydrogel in the surface and pore properties in the hydrogel-coated Fe_3O_4 magnetite composite

The surface area of the hydrogel-coated Fe_3O_4 magnetite composite was found to be 19.78 m^2/g and the pore volume in the hydrogel-coated Fe_3O_4 magnetite composite was found to be 0.1194 cm^3/g for the molar ratio of 1/3 in the iron(II) chloride tetrahydrate and iron(III) chloride hexahydrate to hydrogel (data not shown). In the molar ratios of 1/2, 1/4 and 1/5 for iron(II) chloride tetrahydrate and iron(III) chloride hexahydrate to hydrogel the surface areas and the pore volumes were found smaller than the molar ratio of 1/3 (data not shown). With very low- and high-Fe_3O_4 dopant amount, the photodegradation rate descended gradually because very low and excess doping reduces the mobility of the charge carriers which increases the surface recombination rate resulting in a shortened life span of the hydroxyl radicals. Hydrogel-coated Fe_3O_4 magnetite composite with a molar ratio of 1/3 has a great influence on the photocatalytic activity. At the molar ratio of 1/3, the catalyst may have the fastest transfer of the photo-induced carriers and lowest recombination of electron–holes pairs. Furthermore, the pores present in the hydrogel-coated

Table 1
Characterization values of OMW (n = 3, mean values ± SD)

Parameters	Values		
	Minimum	Medium	Maximum
pH_0	4 ± 0.14	4.4 ± 0.154	4.8 ± 0.168
DO_0 (mg/l)	0.01 ± 0.0004	0.06 ± 0.0021	0.11 ± 0.004
ORP (mV)	122 ± 4.27	128.5 ± 4.98	135 ± 4.725
TSS (mg/l)	55.1 ± 1.93	57.65 ± 2.02	60.2 ± 2.11
COD_{total} (mg/l)	99,130 ± 3,469.6	112,270 ± 3,930	125,410 ± 4,389.4
COD_{dis} (mg/l)	87,200 ± 3,052	102,275 ± 3,579.63	117,350 ± 4,107.3
COD_{inert} (mg/l)	32,460 ± 1,136.1	57,230 ± 2,003.1	82,000 ± 2,870
BOD_5 (mg/l)	64,500 ± 2,257.5	82,030 ± 2,871.1	99,560 ± 3,484.6
BOD_5/COD_{dis}	0.3 ± 0.011	0.6 ± 0.021	0.9 ± 0.032
Total N (mg/l)	198 ± 6.93	259 ± 9.07	320 ± 11.2
NH_4-N (mg/l)	25.2 ± 0.882	32.2 ± 1.13	39.1 ± 1.37
NO_3-N (mg/l)	42 ± 1.5	55 ± 1.93	68 ± 2.4
NO_2-N (mg/l)	19.3 ± 0.7	24.2 ± 0.9	29.1 ± 1.02
Total P (mg/l)	496 ± 17.4	638.7 ± 22.4	781.4 ± 27.4
PO_4-P (mg/l)	352 ± 12.32	456.1 ± 15.96	560.1 ± 19.61
Phenol metabolites (mg/l)			
Catechol	3 ± 0.11	16 ± 0.56	29 ± 1.02
4-methyl catechol	7 ± 0.3	19 ± 0.67	31 ± 1.09
2-PHE	2 ± 0.07	5 ± 0.2	8 ± 0.3
3-PHE	2 ± 0.07	9 ± 0.32	16 ± 0.6
TAAs (mg/l)	1,240 ± 43.4	1,905 ± 67	2,570 ± 90
Individual TAAs (mg/l)			
2,4,6 trimetylalanin	49 ± 1.72	120 ± 4.2	190 ± 6.7
Aniline	42 ± 1.5	108 ± 3.8	174 ± 6.1
o-toluidine	27 ± 0.95	94 ± 3.3	161 ± 5.64
o-anisidine	48 ± 1.7	92 ± 3.22	135 ± 4.73
Dimethylalanine	11 ± 0.4	51 ± 1.8	90 ± 3.2
Ethylbenzene	20 ± 0.7	71 ± 2.5	122 ± 4.3

Notes: SD: standard deviation; n: the repeat number of experiments in this study.

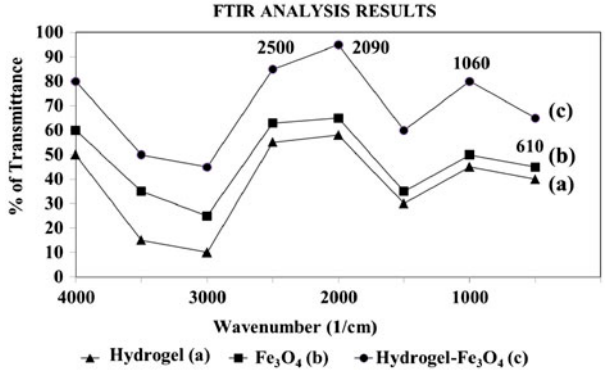

Fig. 2. FTIR analysis results for hydrogel (a), Fe_3O_4 nanoparticles (b), and hydrogel-coated Fe_3O_4 magnetite composites (c).

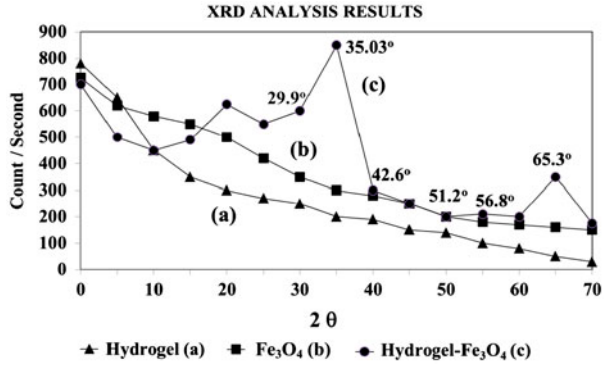

Fig. 3. XRD analysis results for hydrogel (a), Fe_3O_4 nanoparticles (b), and hydrogel-coated Fe_3O_4 magnetite composites (c).

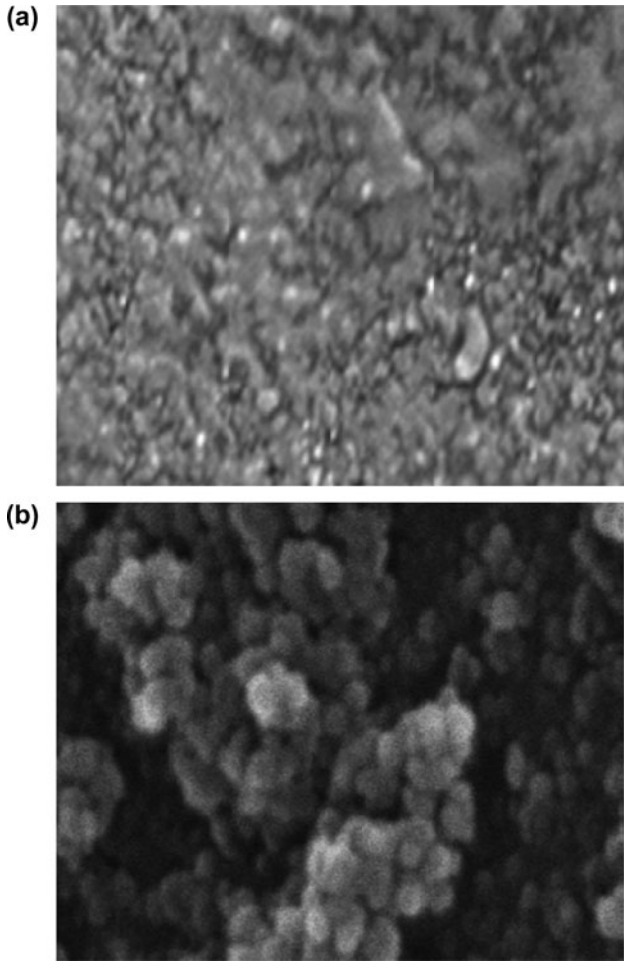

Fig. 4. SEM analysis results for hydrogel-coated Fe_3O_4 magnetite composites (a) without photocatalytic treatment and (b) after photocatalytic treatment of OMW.

Fe_3O_4 magnetite composite at this ratio may allow rapid diffusion of the pollutant molecules during photocatalytic reaction and enhance the adsorption of pollutants (polyphenols, TAAs metabolites, COD components) in the OMW and its intermediates on the catalyst surface. Therefore, all studies were conducted at molar ratio of 1/3 in the iron(II) chloride tetrahydrate and iron(III) chloride hexahydrate to hydrogel in the hydrogel-coated Fe_3O_4 nanocomposite with the exception of temperature run.

3.4. *Effect of different hydrogel-coated Fe_3O_4* magnetite *composite concentrations on the yields of OMW*

The rate of photocatalytic reaction and the removals of pollutants in the OMW are strongly influenced by the amount of the photocatalyst. Generally, in any given photocatalytic application, the optimum catalyst concentration must be determined in order to avoid excess usage of catalyst and to ensure the total absorption of efficient photons. Among the retention times used (10, 20, 30, 60, 75, 120, and 180 min), it was found that the maximum removal efficiencies was observed at 60 min retention time during experimental studies (data not shown). Low contact times cannot be enough for OH radical production throughout photo-oxidation process while high contact times could have decomposed the structure and the pores of hydrogel-coated Fe_3O_4. Therefore, the experimental retention time was selected as 60 min for all experimental conditions. Four different hydrogel-coated Fe_3O_4 magnetite composites concentrations (1, 3, 5, and 7 g/l) were used to determine the maximum yields in the OMW under photocatalytic degradation at 100 W UV irradiation (Table 2). The maximum photodegradation yields were obtained at 3-g/l hydrogel-coated Fe_3O_4 magnetite composites concentration at 100 W UV irradiation after 60 min retention time, at pH 4.0, which is the original pH level of raw OMW (Table 2). The maximum COD_{total}, polyphenols, and TAAs metabolites yields in the OMW were 96%, were between 88 and 94%, and between 83 and 94%, respectively, at 3-g/l of hydrogel-coated Fe_3O_4 magnetite composites, at 100 W UV light irradiation, at pH 4.0, after 60 min retention time, respectively (Table 2).

The effect of varying amount of hydrogel-coated Fe_3O_4 magnetite composite on the pollutants degradation in the OMW shows the variation of percentage photodegradation of COD_{total}, polyphenol, and TAAs metabolites as a function of catalyst concentration. At lower hydrogel-coated Fe_3O_4 magnetite composite levels such as 1-g/l, photonic adsorption controls the extent of reaction due to the limited availability of the hydrogel-coated Fe_3O_4 magnetite composite surface area and catalytic sites. Degradation increases with an increase in the catalyst nanocomposite concentration up to an optimum concentration. The photodegradation reaches up to a maximum of 96% for COD_{total} and a mean of 91% for polyphenols in the initial catalyst loading of 3 g/l. Further increase in the hydrogel-coated Fe_3O_4 magnetite composite concentration showed a negative effect. The decrease in the removal rate beyond the hydrogel-coated Fe_3O_4 magnetite composite concentration of 5.0–7.0 g/l may be attributed to an increase in the turbidity of the suspension since there is a decrease in the UV light penetration as a result of increased scattering effect and hence the photoactivated volume of suspension decreases as reported by Liu et al. [25].

The effect of pollutant concentrations in the OMW was studied both in the presence of UV light and solar light. The maximum COD_{total}, polyphenols, and TAAs

Table 2
Effect of increasing hydrogel-coated Fe_3O_4 magnetite composite concentrations on OMW at 100 W UV and under 29 W sunlight irradiations for 60 min, at pH 4.0 at 21˚C

Parameters (mg/l)	Removal efficiencies (%)							
	UV light irradiation Hydrogel-coated Fe_3O_4 magnetite composite conc. (g/l)				Sunlight irradiation Hydrogel-coated Fe_3O_4 magnetite composite conc. (g/l)			
	1 g/l	3 g/l	5 g/l	7 g/l	1 g/l	3 g/l	5 g/l	7 g/l
COD_{total}	56	96	52	45	51	85	50	42
COD_{dis}	59	95	62	40	53	80	55	38
COD_{inert}	23	67	34	26	20	62	31	24
Total phenol	60	88	60	34	56	83	57	32
Polyphenols								
2-PHE	58	89	56	32	54	85	51	30
3-PHE	60	94	58	36	55	90	54	34
Catechol	60	88	55	32	56	79	50	29
4-methyl catechol	54	90	45	37	50	84	42	33
TAAs	82	94	70	63	80	92	62	60
TAAs metabolites								
Trimethlyaniline	57	87	62	40	54	82	60	35
Aniline	56	85	60	45	52	80	57	42
o-toluidine	60	83	58	48	57	78	53	44
o-anisidine	58	92	45	44	52	87	41	40
Dimethylaniline	58	93	43	56	53	88	40	37
Ethylbenzene	60	92	50	58	56	84	47	38

Notes: COD_{total}: total chemical oxygen demand (mg/l); COD_{dis}: dissolved chemical oxygen demand (mg/l); COD_{inert}: inert chemical oxygen demand (mg/l); 2-PHE: 2-phenyl-phenol (mg/l); 3-PHE: 3-phenyl-phenol (mg/l); TAAs: total aromatic amines (mg/l).

metabolites yields in the OMW under 29 W sunlight irradiation were 85%, between 79 and 90%, between 78 and 92%, respectively, at 3 g/l hydrogel-coated Fe_3O_4 magnetite composite, at pH 4.0, after 60 min retention time, respectively (Table 2). The photocatalytic yields in the OMW parameters at different hydrogel-coated Fe_3O_4 magnetite composite concentrations, at 100 W UV light irradiation were higher than the yields of the OMW at different hydrogel-coated Fe_3O_4 magnetite composite concentrations, at 29 W sunlight irradiation (Table 2). In the presence of UV light, for 125,410 mg/l COD_{total}, 781.4 mg/l total polyphenols, and 2,570 mg/l TAAs, 96, 88, and 94% phtodegradation efficiencies, respectively, occurred within 60 min. However, for the same initial concentration, the degradation reaction was completed within 60 min with the decrease in COD_{total}, polyphenols, and TAAs by 11, 5% and by 2%, respectively, at sunlight irradiation. UV light can produce more electron–hole pairs than visible light; therefore, the efficiency of degradation under UV light irradiation was expected to be better than that under visible light irradiation.

3.5. Effect of different pH values on the yields of OMW

The pH of the wastewater is one of the most important parameter involved in the degradation of aqueous OMW. The effect of pH on the photodegradation of OMW pollutants in the presence of hydrogel-coated Fe_3O_4 magnetite composite particles was investigated over a pH range of 4.0–10.0.The influence of initial pH generally depends on the type of compound that has to be degraded and the zero point charge (ZPC) of the photocatalyst used in the oxidation process [26]. The pH of the OMW influences the surface charge properties of the photocatalyst and increases the electrostatic interaction between the nanocatalyst surface and the organic pollutant molecules. Table 2 illustrates the effect of pH on the initial rate of photocatalytic degradation of COD, TAAs, and polyphenols in the presence of the hydrogel-coated Fe_3O_4

magnetite composite under 100 W UV and 29 W sunlight irradiations. The maximum biodegradation yields for all parameters in the OMW under photocatalytic degradation at UV and sun light irradiations were found at pH 4.0 which this is the original pH level of raw OMW (Table 3). Lower pH may facilitate protonation of amino groups, phenolic and carboxyl groups in which could enhance the adsorption of pollutants by photocatalytic interaction. The pollutants had to compete with the proton for photocatalysis and the protonated functional groups hindered the interaction between the photocatalys and pollutants. This improves the photocatalytic degradation.

In the presence of the aforementioned nanocomposite, the initial percentage degradation of COD, polyphenols and TAAs were found to decrease with the increase in pH from 4.0 up to 7.0 and 10.0. Under alkaline and neutral pHs, the percentage degradation was found to be almost the same (55–65%). At acidic pH values, COD, polyphenols and TAAs exist as positively charged species. The 2-PHE, catechol, 4-methyl catechol metabolite yields were between 86 and 93%, while for o-toluidine, o-anisidine, dimethylalanine TAAs metabolite the yields were between 87 and 93% yields, respectively, in the OMW, under UV light irradiation, at pH 4.0, respectively. Therefore, the photodegradation of carboxcyl groups, of polyphenols and TAAs on the hydrogel-coated Fe_3O_4 magnetite composite surface increase at pH 4.0. However, at pH 10.0, a decrease in the degradation rate is observed which may be due to the higher concentration of the hydroxyl ions (OH^-). Low-degradation rate at higher pH is attributed to the fact that when the concentration of OH^- ion is higher in the solution, it prevents the penetration of UV light to reach the catalyst surface. High pH favors the formation of carbonate ions, which are effective scavengers of OH^- ions, and reduce the pollutant removal rates. Furthermore, at pH 10, the phenolic −OH and aromatic amine −OH and carboxyl groups do not dissociate their protons and hence pollutants attains even higher positive charges cause decreasing photooxidation (Liu et al. [25]). Therefore, COD, polyphenols and TAAs degradations are more favorable in acidic pH than the alkaline and neutral pH on the surface of hydrogel-coated Fe_3O_4 magnetite composite.

Table 3
Effect of increasing pH levels on the yields of the pollutants in the OMW at 3 g/l hydrogel-coated Fe_3O_4 magnetite composite at 100 W UV and under 29 W sun light irradiations after 60 min, at pH 4.0 at 21°C

	Removal efficiencies (%)					
	UV light irradiation pH values			Sunlight irradiation pH values		
Parameters (mg/l)	pH 4.0	pH 7.0	pH 9.0	pH 4.0	pH 7.0	pH 9.0
COD_{total}	96	70	59	84	68	54
COD_{dis}	97	67	60	90	63	58
COD_{inert}	67	66	56	63	62	53
Total phenol	90	73	64	88	70	60
Polyphenols						
2-PHE	86	67	56	83	62	51
3-PHE	84	74	58	81	71	53
Catechol	89	73	55	85	69	50
4-methyl catechol	93	73	45	91	72	42
TAAs	91	68	42	89	64	40
TAAs metabolites						
Trimethlyaniline	85	69	62	82	66	61
Aniline	85	77	65	81	72	63
o-toluidine	93	70	62	90	67	60
o-anisidine	89	65	45	83	61	43
Dimethylaniline	92	69	48	90	65	45
Ethylbenzene	82	66	54	80	62	52

The maximum COD_{total}, polyphenols, and TAAs metabolite yields in the OMW were 93%, between 84 and 93%, between 82 and 93%, respectively, at pH 4.0, under 100 W UV light irradiation, after 60 min retention time, respectively (Table 3). The COD_{total}, polyphenols and TAAs metabolites yields in the OMW under 29 W sunlight irradiation were 84%, between 81 and 91%, between 80 and 90%, respectively, at pH 4.0, after 60 min retention time, respectively (Table 3).

3.6. Effect of reaction temperature on the effectiveness of photodegradation of OMW pollutants with hydrogel-coated Fe_3O_4 magnetite composite under UV irradiation

When the hydrogel-coated Fe_3O_4 magnetite composite concentration was 3 g/l the reactor temperature was changed between 21˚C (room temperature), 30 and 40˚C. Furthermore, the effects of the molar ratio of 1/2, 1/3, 1/4, and 1/5 in the iron(II) chloride tetrahydrate and iron(III) chloride hexahydrate to hydrogel on the pollutant removals in the OMW were investigated at increasing temperatures.

Increase in the reaction temperature improves the photodegradation efficiency. Although collision frequency is greater at higher temperatures, this alone contributes only a very small proportion to the increase in rate of reaction. Much more important is the fact that the proportion of reactant molecules with sufficient energy to react is significantly higher. However, in this study the pollutant photodegradation removals in the OMW increased slightly with temperature increase (Table 4). The best temperature was found to be 40˚C, at this temperature the maximum COD, polyphenols and TAAs efficiencies at the optimum retention time of 60 min were 98, 97, and 97%, respectively, at the molar ratio of 1/3 in the iron(II) chloride tetrahydrate and iron(III) chloride hexahydrate to hydrogel. As shown in Table 4, the maximum photodegradation yield is not always obtained at the maximum temperature; it depends on the molar ratio of the iron(II) chloride tetrahydrate and iron(III) chloride hexahydrate to hydrogel. At the lowest molar ratio of 1/5 in the iron(II) chloride tetrahydrate and iron(III) chloride hexahydrate to hydrogel, the highest photodegradation obtained at 30˚C. Increasing the molar ratio of the iron(II) chloride tetrahydrate and iron(III) chloride hexahydrate to hydrogel (1/3) content shifts the maximum photodegradation yields to be at 40˚C. Here, existed an optimal magnetite content (molar ratio) and temperature to achieve the highest photocatalytic activity. If the concentration of magnetite is too low, the promotional effect is not significant, while for high magnetite content, the active sites of hydrogel-coated Fe_3O_4 magnetite composite may be blocked and lower catalytic activity would be obtained.

As aforementioned, besides enhancing the activation energy, increase the temperature to 40˚C leads to increase slightly the kinetic energy of the pollutants in the OMW which modifies the collisions of the hydrogel-coated Fe_3O_4 magnetite composite surface as reported by Bakarat et al. [27]. If the catalyst surface is very active so numerous free radicals will be present in the surrounding of the catalyst nanoparticles, so fast cracking reactions of the pollutant molecules will take place. The surface is not active relatively at low temperature (21˚C). Increase in the temperature leads to escape the molecules (See Table 4).

3.7. Effect of increasing H_2O_2 concentrations on the yields of the pollutants in the OMW throughout photocatalysis

Table 5 shows the change in degradation percentage on the yields of OMW by varying the amount of H_2O_2 concentration at pH 4.0 at optimum hydrogel-coated Fe_3O_4 magnetite composite loading of 3 g/l with 100 W UV and 29 W sun light irradiations. Four different H_2O_2 concentrations (50, 100, 200, and 1,000 mg/l) was examined for the photodegradation of the OMW under photocatalytic degradation at optimum retention time of 60 min, at pH 4.0. The maximum COD_{total}, polyphenols, and TAAs metabolites yields in the OMW were 94%, between 86 and 94%, between 85 and 96%, respectively, at H_2O_2 = 50 mg/l at 3 g/l hydrogel-coated Fe_3O_4 magnetite composite under 100 W UV light irradiation, at pH 4.0, after 60 retention time (Table 4**).** In this study, the optimum H_2O_2 concentration for the degradation of COD, polyphenols, and TAAs was found to be 50 mg/l in the OMW. COD_{total}, polyphenols, and TAAs metabolites yields in the OMW under 29 W sunlight irradiation were 92%, between 82 and 91%, between 83 and 94%, respectively, at H_2O_2 = 50 mg/l concentration, at 29 W sunlight irradiation, at pH 4.0, after 60 retention time, respectively (Table 5).

The role of added H_2O_2 is different depending on its concentration as reported by Kaur and Singh [28]. At a low concentration of H_2O_2, it increases the formation rate of $OH^{\cdot}$ radical by acting as an electron donor, by reduction of H_2O_2 at the conduction band (CB) and via self decomposition by illumination. However, at a high concentration, H_2O_2 adsorbed on the hydrogel-coated Fe_3O_4 magnetite composite surface could effectively scavenge not only the hydrogel-coated Fe_3O_4 nanocomposite surface-formed $OH^{\cdot}$ radicals but also

Table 4
Effects of temperature increasing on the photodegradation of OMW pollutants according to molar ratio of the iron(II) chloride tetrahydrate and iron(III) chloride hexahydrate to hydrogel in the 3 g/l hydrogel-coated Fe_3O_4 magnetite composite concentration after 60 min retention time under UV light irradiation

Parameters	Removal efficiencies (%)											
	100 W UV light irradiation Hydrogel-coated Fe_3O_4 magnetite composite conc. (3 g/l)											
	Molar ratio of the iron(II) chloride tetrahydrate and iron(III) chloride hexahydrate to hydrogel								Molar ratio of the iron(II) chloride tetrahydrate and iron(III) chloride hexahydrate to hydrogel			
Molar ratios	1:2		1:3		1:4		1:5		1:2	1:3	1:4	1:5
Temperature (°C)	21	30	21	30	21	30	21	30	40	40	40	40
COD_{total}	56	63	96	97	62	63	45	94	99	98	50	42
COD_{dis}	59	63	95	96	56	57	40	93	99	98	55	38
COD_{inert}	23	45	67	68	34	36	26	71	74	73	31	24
Total phenol	60	65	88	89	60	63	34	95	93	92	57	32
Polyphenols												
2-PHE	58	60	89	90	56	58	32	92	93	92	51	30
3-PHE	60	62	94	95	58	60	36	92	98	97	54	34
Catechol	60	62	88	89	55	58	32	92	93	92	50	29
4-methyl catechol	54	56	90	91	45	50	37	90	94	92	42	33
TAAs	82	83	94	95	70	73	63	89	98	97	62	60
TAAs metabolites												
Trimethlyaniline	57	60	87	88	62	63	40	88	90	90	60	35
Aniline	56	60	85	87	60	62	45	89	90	88	57	42
o-toluidine	60	64	83	85	58	63	48	86	90	88	53	44
o-anisidine	58	62	92	93	45	51	44	88	96	94	41	40
Dimethylaniline	58	61	93	94	43	47	56	90	96	95	40	37
Ethylbenzene	60	63	92	93	50	54	58	90	97	96	47	38

the photogenerated hole, which can inhibit the major pathway for generation of $OH^{\cdot}$ radicals.

The addition of H_2O_2 into the photocatalytic system was expected to promote the degradation of pollutants in the OMW. But, exceeding the optimum dosage (>50 mg/l H_2O_2) would trap the $OH^{\cdot}$ to form weaker oxidant hydroperoxyl radicals ($O_2H^{\cdot}$). Accordingly, the capture of $OH^{\cdot}$ was occurred through Eqs. (1) and (2), as follows:

$$H_2O_2 + OH^{-\cdot} \rightarrow H_2O + O_2H^{\cdot} \quad (1)$$

$$O_2H^{\cdot} + OH^{-\cdot} \rightarrow H_2O + O_2 \quad (2)$$

The decline in the $OH^{\cdot}$ concentration, trigged by the higher H_2O_2 dosage, decreased the degradation of pollutants in the OMW. At optimum H_2O_2 concentration the photochemical reduction of Fe(III)-complex coupled to the H_2O_2 reaction. The production of oxidative species, such as superoxide ($O_2^{\cdot -}$), $O_2H^{\cdot}$ and $OH^{\cdot}$ radicals, the utilization of iron oxides, and hydrogel to produce $OH^{\cdot}$ without addition of external amounts of H_2O_2 and Fe.

3.8. Photocatalysis mechanism of pollutants in the OMW with hydrogel-coated Fe_3O_4 magnetite composites

The mechanism of photodegradation of polyphenols, COD, and TAAs on hydrogel-coated Fe_3O_4 magnetite composite surface were as follows: the excitation of hydrogel-coated Fe_3O_4 magnetite composite by solar energy leads to the formation of an electron–hole pair. The hole combines with water (H_2O) to form hydroxyl radicals ($OH^{\cdot}$), while electron converts oxygen (O_2) to superoxide radical ($O_2^{\cdot -}$), a strong oxidizing species as shown below (Eqs. (3)–(7)):

Table 5
Effect of increasing H_2O_2 concentrations on the yields of the pollutants in the OMW, at 100 W UV and under 29 W sunlight irradiations after 60 min, at pH 4.0 at 21°C

	Removal efficiencies (%) UV light irradiation H_2O_2 concentrations (mg/l)				Sunlight irradiation H_2O_2 concentrations (mg/l)			
Parameters (mg/l)	50 mg/l	100 mg/l	200 mg/l	1,000 mg/l	50 mg/l	100 mg/l	200 mg/l	1,000 mg/l
COD_{total}	98	90	78	57	92	88	75	54
COD_{dis}	97	85	74	45	90	82	71	43
COD_{inert}	72	62	51	33	67	60	50	31
Total phenol	97	86	77	54	91	82	73	52
Polyphenols								
2-PHE	94	70	57	39	85	68	54	37
3-PHE	95	68	55	37	82	64	51	35
Catechol	92	84	68	55	89	81	63	51
4-methyl catechol	94	86	71	62	91	83	67	60
TAAs	94	85	70	61	90	82	69	59
TAAs metabolites								
Trimethlyaniline	94	80	64	56	84	79	62	55
Aniline	94	79	63	54	85	77	60	52
o-toluidine	96	84	72	65	94	81	70	62
o-anisidine	93	79	66	58	88	76	64	55
Dimethylaniline	95	82	71	64	92	79	68	61
Ethylbenzene	95	67	56	41	83	62	52	39

hydrogel-coated Fe_3O_4 magnetite composite $+ h\nu \rightleftharpoons$ hydrogel-coated Fe_3O_4 magnetite composite $+ h^+_{VB} + e^-_{CB}$ (3)

hydrogel-coated Fe_3O_4 magnetite composite $|OH^- + h^+_{VB} \rightarrow$ hydrogel-coated Fe_3O_4 magnetite composite $|OH^{\cdot}$ (4)

hydrogel-coated Fe_3O_4 magnetite composite $|OH_2 + h^+_{VB} \rightarrow$ hydrogel-coated Fe_3O_4 magnetite composite $|OH^{\cdot} + H^+$ (5)

hydrogel-coated Fe_3O_4 magnetite composite$|OH^{\cdot} + Red_{org} \rightarrow Ox_{org} \rightarrow$ photo − degradation of OMW pollutants (6)

$h^+_{VB} + Red_{org} \rightarrow Ox_{org} \rightarrow$ photo − degration of OMW pollutants (7)

COD, polyphenols and TAAs are degraded via photooxidation process by reacting with both $OH^{\cdot}$ radicals and h^+_{VB} according to Eqs. (3)–(5). The $OH^{\cdot}$ shows electrophilic character and prefers to attack electron rich ortho or para carbon atoms of COD, polyphenols and TAAs. This results in the formation of polyphenol metabolites (catechol, tyrosol, quercetin, caffeic acid, 4-methyl catechol, 2-PHE, 3-PHE) from total phenol and TAAs metabolites {2,4,6-trimetylalanin, aniline, o-toluidine, o-anisidine, dimethylalanine, ethylbenzene, durene [3,6-bis (dimethylamino)]} from TAAs are formed with photodegradation process in the OMW under UV and sun light irradiation, respectively.

When hydrogel-coated Fe_3O_4 magnetite composites irradiated with light energy equal to or higher than its band gap, an electron (e^-) can be excited from the valence band (VB) to the CB and leaving a hole (h^+) in the VB [17]. If charge separation is maintained, the paired $e^- - h^+$ may migrate to the surface of the photocatalyst. In aqueous phase, the photo induced h^+ is apparently able to oxidize surface OH groups or surface-bond H_2O to produce highly reactive and nonselective $OH^{\cdot}$. The $OH^{\cdot}$ are considered to be the dominant oxidizing species contributing to the photocatalytic degradation of organic substrates [13].

The reaction of Fe_3O_4 during photocatalysis is as follows (Eqs. (8)–(10)):

$$Fe^{3+} + O_2^{\cdot -} \rightarrow Fe^{2+\cdot} + O_2 \quad (8)$$

$$O_2^{\cdot -} + nH^+ + Fe^{2+} \rightarrow Fe^{3+} + H_2O_2 \quad (9)$$

$$Fe^{2+} + H_2O_2 \rightarrow Fe^{3+} + OH^- + OH^{\cdot} \quad (10)$$

According to this mechanism, photolysis of Fe(III)—hydrogel complexes forms H_2O_2, Fe^{+3} can result in the radical chain mechanism. Higher photocatalytic activity of hydrogel-coated Fe_3O_4 magnetite composite nanoparticles in the degradation of organics has been reported [29]. The fact can be related to the vectorial transfer of electrons and holes, which takes place in different redox energy levels, for their corresponding CB and VB. When the hydrogel-coated Fe_3O_4 magnetite composite nanoparticles are agitated by photons with energy higher than the band gap energy (Eg), large number of electrons get promoted from VB to the CB of hydrogel-coated Fe_3O_4 magnetite composites, leading to the generation of electron/hole (e^-/h^+) pairs [26]. The electrons transfer from the CB of hydrogel-coated Fe_3O_4 magnetite composites to the VB of hydrogel-coated Fe_3O_4 magnetite composites decreasing the pairs' recombination rate as reported by Rao et al. [30].

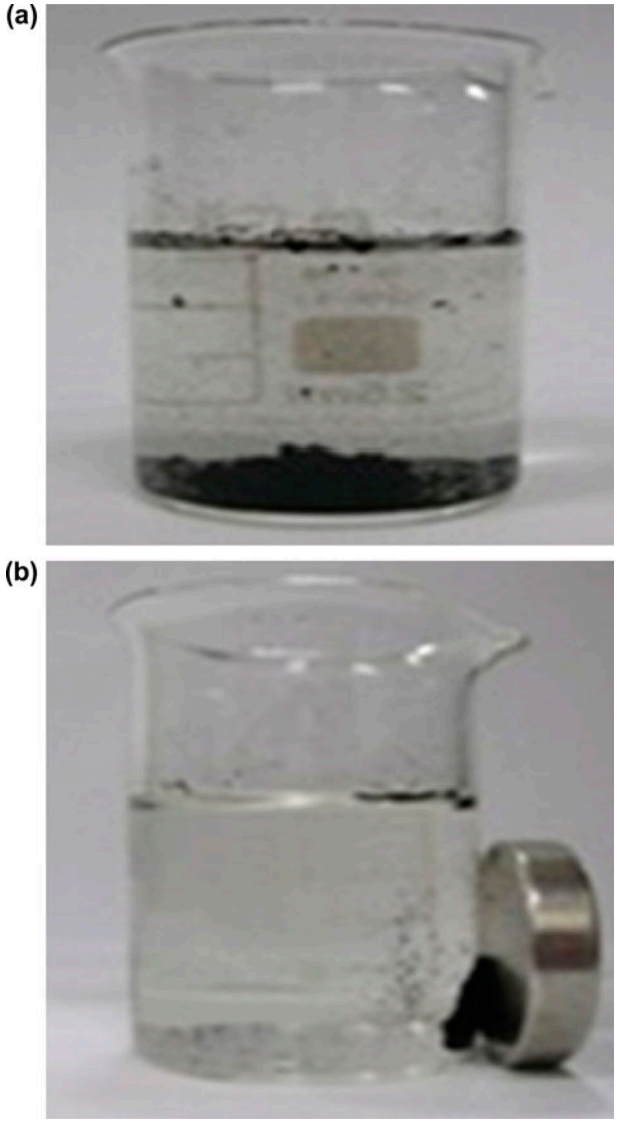

Fig. 5. Recovery of hydrogel-coated Fe_3O_4 magnetite composites with magnetic separation process after biodegradation of the OMW under photocatalytic degradation (UV and sunlight irradiation) (a) before magnetic separation process and (b) after magnetic separation process.

3.9. Recovery of hydrogel-coated Fe_3O_4 magnetite composites

Magnetic separation provides a very convenient approach for removing and recycling magnetic composites by applying an added magnetic field. The separation of Fe_3O_4 from the hydrogel-coated Fe_3O_4 magnetite composite in the OMW becomes very easy owing to the superparamagnetic nature of Fe_3O_4 nanoparticles at room temperature. In the magnetic separation technique, the hydrogel-coated Fe_3O_4 magnetite composite became adsorbed onto the magnetic stirring bar when the stirring was stopped. In our experiments, the stability and reusability of the photocatalyst were examined by repetitive use of the catalyst (data not shown). After the pollutants in the OMW were photodegraded in the hydrogel-coated Fe_3O_4 magnetite composite was washed with H_2O and were cleaned with 34% ethanol and 45% butanol for 30 min. It is separated using a simple bar magnet and dried at 200°C for 2 h and then was added again into the same concentration was almost as yield as in the first run (94% for COD_{total}, 86% for polyphenols and 92% for TAAs) (data not shown). Repeatedly, the four runs of the degradation of COD_{total}, polyphenols, and TAAs showed no significant loss of photoactivity of the hydrogel-coated Fe_3O_4 magnetite composite, which indicated the considerable stability of the hydrogel-coated Fe_3O_4 magnetite composite under the present conditions.

Fig. 5(a) illustrated the recovery of hydrogel-coated Fe_3O_4 magnetite composites with magnetic separation process after photodegradation of pollutants in the OMW under photocatalytic degradation (UV and sun light irradiation) before magnetic separation process, and after magnetic separation process in Fig. 5(b). The hysteresis loops tests and the saturation magnetization of the magnetic hydrogel-coated Fe_3O_4 magnetite composites was not measured.

4. Conclusions

The maximum COD components, polyphenol, and TAAs yields in the OMW were obtained at 3 g/l of hydrogel-coated Fe_3O_4 magnetite composites, at acidic pH, after 60 min İrradiation time at 50 mg/l H_2O_2 concentration and at the lowest molar ratio of 1/5 in the iron(II) chloride tetrahydrate and iron(III) chloride hexahydrate to hydrogel at 30˚C and at a molar ratio of 1/2 in the iron(II) chloride tetrahydrate and iron (III) chloride hexahydrate to hydrogel at 40˚C under UV and solar light irradiatons. The pollutant yields obtained under 100 W UV irradiation is higher than the yields obtained under 29 W solar irradiation. Fe_3O_4 exhibited high catalytic recyclability from the hydrogel-coated Fe_3O_4 magnetite composites. This decrease the cost spent for the treatment of OMW which is a highly pollutant wastewater and could not be treated effectively with the conventional and other advanced treatment technologies.

In conclusion, the fast and sustainable removable of pollutants (polyphenols, COD components, TAAs) from the OMW is possible with hydrogel-coated Fe_3O_4 magnetite composites under photodegradation process under UV and sunlight irradiations. The yields of all experimental parameters under 100 W UV light irradiation in the OMW during photocatalytic degradation process were higher than the yields of all experimental parameters under 29 W sunlight irradiation.

Acknowledgments

This research study was undertaken in the Environmental Microbiology Laboratury at Dokuz Eylül University Engineering Faculty Environmental Engineering Department, İzmir, Turkey.

References

[1] O.S. Ekici, Y. Baran, N. Aktas, N. Sahiner, Removal of toxic metal ions with magnetic hydrogels, Water Res. 43 (2009) 4403–4411.
[2] E. Ramírez, S.G. Burillo, C. Barrera-Díaz, G. Roa, B. Bilyeu, Use of pH sensitive polymer hydrogels in lead removal from aqueous solution, J. Hazard. Mater. 192 (2011) 432–439.
[3] A. Acarregui, J.L. Pedraz, F.J. Blanco, R.M. Hernández, G. Orive, Hydrogel-based scaff olds for enclosing encapsulated therapeutic cells, Biomacromolecules 14 (2013) 322–330.
[4] V.H. Luan, H.N. Tien, L.T. Hoa, N.T.M. Hien, E.-S. Oh, J.S. Chung, E.J. Kim, W.M. Choi, B.-S. Kong, S.H. Hur, Synthesis of a highly conductive and large surface area graphene oxide hydrogel and its use in a supercapacitor, J. Mater. Chem. A 1 (2013) 208–211.
[5] L. Yan, Z. Zhu, Y. Zou, Y. Huang, D. Liu, S. Jia, D. Xu, M. Wu, Y. Zhou, S. Zhou, C.J. Yang, Target-responsive "sweet" hydrogel with glucometer readout for portable and quantitative detection of non-glucose targets, J. Am. Chem. Soc. 135 (2013) 3748–3751.
[6] K. Kesenci, R. Say, A. Denizli, Removal of heavy metal ions from water by using poly(ethyleneglycol dimethacrylate-co-acrylamide) beads, Eur. Polym. J. 38 (2002) 1443–1448.
[7] H.A. Essawy, H.S. Ibrahim, Synthesis and characterization of poly(vinylpyrrolidone-co-methylacrylate) hydrogel for removal and recovery of heavy metal ions from wastewater, React. Funct. Polym. 61 (2004) 421–432.
[8] M.A. Barakat, N. Sahiner, Cationic hydrogels for toxic arsenate removal from aqueous environment, J. Environ. Manage. 88 (2008) 955–961.
[9] M.A. Barakat, New trends in removing heavy metals from industrial wastewater, Arabian J. Chem. 4 (2011) 361–377.
[10] J.-Y. Sun, X. Zhao, W.R.K. Illeperuma, O. Chaudhuri, K.H. Oh, D.J. Mooney, J.J. Vlassak, Z. Suo, Highly stretchable and tough hydrogels, Nature 489 (2012) 133–136.
[11] K. Haraguchi, Nanocomposite hydrogels: A unique organic–inorganic network structure with extraordinary mechanical, optical, and swelling/de-swelling properties, Adv. Mater. 14 (2002) 1120–1123.
[12] K. Haraguchi, Synthesis and properties of soft nanocomposite materials with novel organic/inorganic network structures, Polym. J. 43 (2011) 223–241.
[13] H. Ren, M. Zhu, K. Haraguchi, Characteristic swelling–deswelling of polymer/clay nanocomposite gels, Macromolecules 44 (2011) 8516–8526.
[14] K. Haraguchi, K. Murata, T. Takehisa, Stimuli-responsive nanocomposite gels and soft nanocomposites consisting of inorganic clays and copolymers with different chemical affinities, Macromolecules 45 (2012) 385–391.
[15] Q. Wang, J.L. Mynar, M. Yoshida, E. Lee, M. Lee, K. Okuro, K. Kinbara, T. Aida, High-water-content mouldable hydrogels by mixing clay and a dendritic molecular binder, Nature 463 (2010) 339–343.
[16] R.A. Frimpong, J.Z. Hilt, Poly(n-isopropylacrylamide)-based hydrogel coatings on magnetite nanoparticles via atom transfer radical polymerization, Nanotechnology 19 (2008) 1–7.
[17] B. Li, D. Jia, Y. Zhou, Q. Hu, W. Cai, *In situ* hybridization to chitosan/magnetite nanocomposite induced by the magnetic field, J. Magn. Magn. Mater. 306 (2006) 223–227.
[18] S.R. Bhattarai, K.C. Remant Bahadur, S. Aryal, K.M.S. Khil, H.Y. Kim, N-Acylated chitosan stabilized iron oxide nanoparticles as a novel nano-matrix and ceramic modification. Carbohyd. Polym. 69 (2007) 467–477.
[19] S. Bao, D. Wu, Q. Wang, T. Su, Functional elastic hydrogel as recyclable membrane for the adsorption and degradation of methylene blue, PLoS ONE 9(2) (2014) e88802, 1–8, doi: 10.1371/journal.pone.0088802.
[20] R. Oztekin, D.T. Sponza, Treatment of wastewaters from the olive mill industry by sonication, J. Chem. Technol. Biotechnol. 88(2) (2013) 212–225.

[21] D.T. Sponza, R. Oztekin, Dephenolization, dearomatization and detoxification of olive mill wastewater with sonication combined with additives and radical scavengers, Ultrason. Sonochem. 21(3) (2014) 1244–1257.
[22] D.T. Sponza, R. Oztekin, Treatment of the olive mill industry wastewater with ultrasound and some nano-sized metal oxides, J. Chem. Eng. Process Technol. 4 147(2) (2013) 1–9.
[23] A.D. Eaton, L.S. Clesceri, E.W. Rice, A.E. Greenberg, M.A.H. Franson, (Eds.), Standard Methods for the Examination of Water and Wastewater. (twenty oneth ed.), American Public Health Association (APHA), AmericanWaterWorks Association (AWWA), Water Environment Federation (WEF), American Public Health Association 800 I Street, NW, Washington, DC, 20001–23770, USA, 2005.
[24] F. Germirli, D. Orhon, N. Artan, Assessment of the initial inert soluble COD in industrial wastewater, Water Sci. Technol. 23 (1991) 1077–1086.
[25] N. Liu, J. Shen, D. Liu, A Fe_2O_3 nanoparticle/carbon aerogel composite for use as an anode material for lithium ion batteries, Electrochim. Acta 97 (2013) 271–277.
[26] K. Samba Sivudu, K.Y. Rhee, Preparation and characterization of pH-responsive hydrogel magnetite nanocomposite. Colloids Surf., A: Physicochem. Eng. Aspects 349(1–3) (2009) 29–34.
[27] N.A.M. Barakat, I.S. Chronakis, H.Y. Kim, Influence of temperature on the photodegradation process using Ag-doped TiO_2 nanostructures: Negative impact with the nanofibers. J. Mol. Catal. A Chem. 366 (2013) 333–340. Available from: <http://www.sciencedirect.-com/science/article/pii/S1381116912003433-cor0005#-cor0005mailto:nasser@jbnu.ac.krM.A. Kanjwal>.
[28] S. Kaur, V. Singh, TiO_2 mediated photocatalytic degradation studies of Reactive Red 198 by UV irradiation, J. Hazard. Mater. 141 (2007) 230–236.
[29] C. Shen, Y. Shen, Y. Wen, H. Wang, W. Liu, Fast and highly efficient removal of dyes under alkaline conditions using magnetic chitosan-Fe(III) hydrogel, Water Res. 45(16) (2011) 5200–5210.
[30] P. Rao, I.M.C. Lo, K. Yin, S.C.N. Tang, Removal of natural organic matter by cationic hydrogel with magnetic properties, J. Environ. Manage. 92(7) (2011) 1690–1695.